J. Fluid Mech. (2008), *vol.* 595, *pp.* 221–237.
doi:10.1017/S0022112007009147 Printed in the United Kingdom

Effect of an electric field on the stability of contaminated film flow down an inclined plane

M. G. BLYTH

School of Mathematics, University of East Anglia, Norwich, NR4 7TJ, UK

(Received 22 January 2007 and in revised form 10 September 2007)

The stability of a liquid film flowing down an inclined plane is considered when the film is contaminated by an insoluble surfactant and subjected to a uniform normal electric field. The liquid is treated as a perfect conductor and the air above the film is treated as a perfect dielectric. Previous studies have shown that, when acting in isolation, surfactant has a stabilizing influence on the flow while an electric field has a destabilizing influence. The competition between these two effects is the focus of the present study. The linear stability problem is formulated and solved at arbitrary parameter values. An extended form of Squire's theorem is presented to argue that attention may be confined to two-dimensional disturbances. The stability characteristics for Stokes flow are described exactly; the growth rates of the normal modes at finite Reynolds number are computed numerically. We plot the neutral curves dividing regions of stability and instability, and trace how the topology of the curves changes as the intensity of the electric field varies both for a clean and for a contaminated film. With a sufficiently strong electric field, the neutral curve for a clean film consists of a lower branch trapping an area of stable modes around the origin, and an upper branch above which the flow is stable. With surfactant present, a similar situation obtains, but with an additional island of stable modes disjoint from the upper and lower branches.

1. Introduction

A voluminous literature has accumulated over the years addressing the flow of single or multi-layered liquid films down an inclined plane (for a review, see Pozrikidis 2004). Much of the interest stems from the many industrial applications of these types of flow. A thorough theoretical understanding of film flow behaviour is crucial in aiding the design or improvement of technologies such as the manufacture of photographic plates (e.g. Kistler & Schweizer 1997), and the development of lab-on-a-chip microdevices (e.g. Karniadakis, Beskok & Aluru 2005) and spinning-disk reactors (e.g. Matar & Lawrence 2006). In applications, the occurrence of waves on the surface of the film may be a desirable feature, as in the case of a cooling film where surface waves enhance heat transport (e.g. Dukler 1976; Yoshimura, Nosoko & Nagata 1996). Conversely, surface waves may be an undesirable feature, as in the case of coating flows where a smooth surface is usually required for the finished product (e.g. Weinstein & Ruschak 2004).

One way to control surface waves on a liquid film is to use surface active agents, or surfactants, which influence the dynamics by lowering the local surface tension. The stability properties of a clean film with no surfactant present were first described by Benjamin (1957) and Yih (1963). At zero Reynolds number, a clean film is stable

to all linear perturbations. However, the flow becomes unstable when the Reynolds number is raised above a critical value. The sufactant contributes an additional term to the tangential stress balance at the film surface and establishes local surface tension gradients and Marangoni tractions. Theoretical work by Benjamin (1964) and Whitaker (1964) showed that surfactant raises the critical Reynolds number for instability and hence tends to stabilize the film. Whitaker & Jones (1966) and Lin (1970) obtained an asymptotic estimate for the critical Reynolds number valid in the limit of long waves. Their result was confirmed by Anshus & Acrivos (1967) for the case of a liquid film flowing down a vertical wall. Ji & Setterwall (1994) identified an unstable Marangoni mode associated with the presence of a soluble surfactant in a vertically falling film. Blyth & Pozrikidis (2004*b*) studied inclined film flow in the presence of an insoluble surfactant and calculated the neutral curve dividing stable and unstable regions for arbitrary Reynolds number and wavenumber. The overall effect of the surfactant is stabilizing; it raises the critical Reynolds number for instability at any given wavenumber. In related work, Frenkel & Halpern (2002), Halpern & Frenkel (2003) and Blyth & Pozrikidis (2004*a*) considered the stability of two-layer flow in the presence of an insoluble surfactant. This work was extended to include inertia by Blyth & Pozrikidis (2004*c*) and by Frenkel & Halpern (2005).

Another means of controlling the dynamics of a liquid film is through the application of an electric field. In theoretical investigations, the film is often regarded as a perfect conductor, wherein the electric field vanishes, and the air above the film is regarded as a perfect dielectric supporting a potential difference between the film surface and, for example, an electrode placed some distance from the wall. The electric field influences the flow by contributing an additional Maxwell stress term to the balance of normal stress at the film surface. Previous work has revealed that the electric field has a generally destabilizing effect on the flow. Using a long-wave theory, Gonzalez & Castellanos (1996) demonstrated that the critical Reynolds number is lowered when the film is electrified. Their work was extended to large Reynolds number by Mukhopadhyay & Dandapat (2005). Tseluiko & Papageorgiou (2006) conducted a long-wave analysis of electrified film flow down an inclined plane and developed an evolution equation to describe the weakly nonlinear dynamics. In an appropriate set of limits, they showed that their equation reduces to the Kuramoto–Sivashinsky equation and demonstrated the existence of periodic travelling waves, homoclinic bursts and chaotic oscillations. Kim, Bankoff & Miksis (1991) investigated film flow down a plane wall when an electrode of finite length is placed at a fixed distance from the wall. They performed linear stability calculations assuming an infinite electrode, and used the lubrication approximation to derive a nonlinear evolution equation for the film height for a finite electrode. Solutions of the film height equation were compared with experimental observations by Griffing *et al.* (2006). The effect of a magnetic field on inclined film flow has also been considered (e.g. Shen, Sun & Meyer 1991).

In the present work, we consider film flow down an inclined plane and focus on the competition between the stabilizing influence of an insoluble surfactant and the destabilizing influence of an electric field. The combined effects of an electric field and a surfactant have been studied in the context of the deformation of a viscous drop (Ha & Yang 1995, 1998). In the current model, the liquid film is assumed to be a perfect conductor, and the air above the film is assumed to be a perfect dielectric. The surfactant is assumed to be insoluble and therefore unable to penetrate the bulk of the fluid. Our aim is to determine the stability of the liquid film over a range of parameter values. In particular, we compute neutral curves in wavenumber/Reynolds

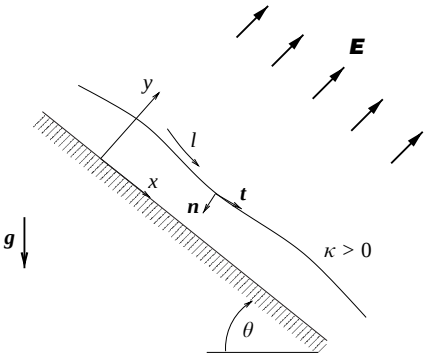

FIGURE 1. Illustration of gravity-driven film flow down an inclined plane wall. The film is contaminated with an insoluble surfactant and an electric field acts normal to the wall at infinity.

number space and demonstrate how their topology changes as the intensity of the electric field or the prevailing level of surfactant is varied.

In § 2, we formulate the general problem of electrified film flow; in § 3, we prepare the equations governing the stability of small perturbations; in § 4, we present solutions to the linear stability problem; and finally, in § 5, we summarize our findings.

2. Problem formulation

We consider the stability of gravity-driven film flow down a plane wall in the presence of an electric field when the film is contaminated with an insoluble surfactant (figure 1). The liquid film is assumed to be a perfect conductor, and the air above the film is assumed to be a perfect dielectric. The electric field at infinity acts in the direction normal to the wall. The surfactant, which is present in the concentration $\Gamma(x, t)$, diffuses and is convected freely over the film surface, but is not able to penetrate the bulk of the fluid. At each point on the surface, the local surface tension $\gamma(x, t)$ varies according to the local surfactant concentration.

The fluid motion in the film satisfies the Navier–Stokes equation and the incompressibility condition,

$$\frac{\partial \boldsymbol{u}}{\partial t} + \boldsymbol{u}\cdot\nabla\boldsymbol{u} = -\frac{1}{\rho}\nabla p + \frac{\mu}{\rho}\nabla^2\boldsymbol{u}, \qquad \nabla\cdot\boldsymbol{u} = 0, \tag{2.1}$$

where ρ and μ are, respectively, the density and viscosity of the liquid, p is the pressure and $\boldsymbol{u} = (u_x, u_y)$ is the velocity. The boundary conditions at the wall are those of no-slip and impermeability. The jump in the fluid stress at the free surface is balanced by the capillary pressure, the Marangoni force due to surfactant-induced variations in the surface tension, and the Maxwell force due to the electric field, so that

$$\boldsymbol{\sigma}\cdot\boldsymbol{n} = -(\gamma\kappa + p_a)\,\boldsymbol{n} - \frac{\partial\gamma}{\partial l}\,\boldsymbol{t} + \boldsymbol{M}\cdot\boldsymbol{n}, \tag{2.2}$$

where l measures arclength along the free surface, p_a is the atmospheric pressure, $\boldsymbol{n}$ is the unit normal to the free surface pointing into the film, and $\boldsymbol{\sigma}$ is the Newtonian stress tensor in the liquid. The curvature, κ, is taken to be positive when the surface is downwards parabolic (figure 1). The Maxwell stress tensor, $\boldsymbol{M}$, is defined by (e.g.

Melcher & Taylor 1969)

$$\boldsymbol{M} = \varepsilon \left(\boldsymbol{E}\,\boldsymbol{E} - \tfrac{1}{2}\boldsymbol{I}\,|\boldsymbol{E}|^2 \right), \tag{2.3}$$

where $\boldsymbol{E}$ is the electric field and ε is the permittivity of the air above the film. Since the fluid is assumed to be a perfect conductor, the electric field at the fluid surface acts only in the normal direction. From (2.2) and (2.3), it follows that the electric field does not contribute to the tangential stress balance at the free surface, which includes only the effect of the surfactant and is given by

$$\mathbf{t}\cdot\boldsymbol{\sigma}\cdot\boldsymbol{n} = -\frac{\partial\gamma}{\partial l}. \tag{2.4}$$

However, it contributes a positive term to the right-hand side of the normal stress balance at the free surface, which is expressed by

$$\boldsymbol{n}\cdot\boldsymbol{\sigma}\cdot\boldsymbol{n} = -(\gamma\kappa + p_a) + \tfrac{1}{2}\varepsilon|\boldsymbol{E}|^2. \tag{2.5}$$

Finally, the kinematic condition at the free surface, located at $y = f(x,t)$, requires that $\mathrm{D}(y-f)/\mathrm{D}t = 0$, where $\mathrm{D}/\mathrm{D}t$ is the material derivative.

Introducing a potential, $\phi(x, y, t)$, such that $\boldsymbol{E} = -\nabla\phi$, the electric field is assumed to satisfy the Laplace equation above the film,

$$\nabla^2\phi = 0. \tag{2.6}$$

Since the liquid is a perfect conductor, the electric field at the film surface must satisfy the condition $\boldsymbol{E}\cdot\boldsymbol{t} = 0$, where $\boldsymbol{t}$ is the unit tangent pointing in the direction of increasing arclength. Accordingly, we take $\phi = 0$ on $y = f(x,t)$. A long way from the film, the electric field acts normal to the wall with strength E so that $\phi \to -E\,y$ as $y \to \infty$.

The surfactant concentration, Γ, satisfies the surface convection–diffusion equation,

$$\frac{\mathrm{d}\Gamma}{\mathrm{d}t} + \frac{\partial(u_t\,\Gamma)}{\partial l} = -\Gamma\,\kappa\,u_n + D_s\frac{\partial^2\Gamma}{\partial l^2}, \tag{2.7}$$

(e.g. Li & Pozrikidis 1997; Yon & Pozrikidis 1998), where $u_t = \boldsymbol{u}\cdot\boldsymbol{t}$ and $u_n = \boldsymbol{u}\cdot\boldsymbol{n}$ are the interfacial velocities in the directions of the tangential and normal vector, respectively, and D_s is the surface surfactant diffusivity. In most practical applications, the surfactant diffusivity is very small. The derivative $\mathrm{d}/\mathrm{d}t$ on the left-hand side of (2.7) denotes the rate of change following the motion of interfacial marker points moving with the component of the fluid velocity normal to the interface (Li & Pozrikidis 1997). Since the electric field acts only in the normal direction at the free surface, there is no component of the electric force in the tangential direction and (2.7) is expected to hold as a first approximation. Accordingly, the electric field is assumed to have only a passive effect on the surfactant transport.

The surfactant is assumed to alter the local surface tension according to Gibbs' linear equation of state, $\gamma_c - \gamma = \Gamma RT$, where R is the ideal gas constant, T is the absolute temperature, and γ_c is the surface tension prevailing in the absence of surfactant (see e.g. Adamson 1990). It is convenient to express this equation in the equivalent form,

$$\gamma = \gamma_c\left(1 - \beta\frac{\Gamma}{\Gamma_0}\right), \tag{2.8}$$

where Γ_0 is the reference level of the surfactant concentration in the unperturbed state of a flat film with corresponding surface tension $\gamma_0 = \gamma_c(1-\beta)$. The dimensionless

parameter $\beta = \Gamma_0 RT/\gamma_c$ is related to the so-called surface elasticity $E = \gamma_c \beta/\Gamma_0$. In this paper, we will present results in terms of the dimensionless Marangoni number, Ma, which is related to β through $Ma = \beta/(1-\beta)$. When $Ma = 0$, the surface tension is constant and the Marangoni force vanishes.

An exact solution of the problem (2.1)–(2.8) valid for a flat film surface is given by the well-known Nusselt profile in the liquid,

$$u_x = \frac{\rho g \sin\theta}{2\mu}\, y(2h - y), \qquad u_y = 0, \qquad p = p_a + \rho g(h - y)\cos\theta, \tag{2.9}$$

where g is the acceleration due to gravity and h is the uniform height of the film, and by

$$\phi = -E\, y \tag{2.10}$$

for the electric potential. In the next section, we shall examine the stability of the basic solution (2.9) and (2.10) to a linear perturbation to the free surface. Our aim is to classify the film stability according to the intensity of the imposed electric field and the prevailing strength of the surfactant.

3. Linear stability

In this section, we perform a linearised analysis to determine the stability of the film to small perturbations. First we nondimensionalise the flow variables using the Nusselt surface speed, $U_s = (\rho g h^2 \sin\theta)/2\mu$, the undisturbed film height, h, the pressure scale ρU_s^2, and the time scale h/U_s. The electric potential is nondimensionalised using the far-field reference value Eh and the surface tension and the surfactant concentration using the reference values γ_0 and Γ_0. All variables presented henceforth have been made dimensionless according to these scales.

In order to assess the stability of the film flow, we appeal to an extended form of Squire's transformation (see Appendix A) and confine our attention to two-dimensional disturbances. Proceeding, we perturb the film height so that the free surface is located at

$$y = 1 + \delta\, A_1\, \mathrm{e}^{\mathrm{i}k(x-ct)}, \tag{3.1}$$

where δ is a small parameter. Introducing a stream function, $\psi(x, y, t)$, defined so that $u = \partial\psi/\partial y$ and $v = -\partial\psi/\partial x$, the solution to the perturbed problem is found at successive levels of approximation by expanding in powers of δ as follows,

$$\left.\begin{aligned} &\psi = y^2\left(1 - \tfrac{1}{3}y\right) + \delta\, \psi_1(y)\, \mathrm{e}^{\mathrm{i}k(x-ct)} + \cdots, \quad \gamma = 1 + \delta\, \gamma_1\, \mathrm{e}^{\mathrm{i}k(x-ct)} + \cdots, \\ &\Gamma = 1 + \delta\, \Gamma_1\, \mathrm{e}^{\mathrm{i}k(x-ct)} + \cdots, \quad \phi = -y + \delta\, \phi_1(y)\, \mathrm{e}^{\mathrm{i}k(x-ct)} + \cdots, \end{aligned}\right\} \tag{3.2}$$

with a similar expansion for the pressure. Substituting into the dimensionless form of (2.1) and linearizing, we derive the Orr-Sommerfeld equation

$$\psi_1^{(\mathrm{iv})} - 2k^2\psi_1'' + k^4\psi_1 = \mathrm{i}kRe\, [(2y - y^2 - c)(\psi_1'' - k^2\psi_1) + 2\psi_1], \tag{3.3}$$

where a prime denotes differentiation with respect to y. To satisfy the no-slip and impermeability conditions, we require that $\psi_1 = \psi_1' = 0$ at $y = 0$. Linearising the dimensionless form of (2.2) and using the linearised dimensionless forms of (2.7) and (2.8), we obtain the condition for the jump in the tangential stress component at

the free surface,

$$\psi_1'' + k^2\psi_1 - 2A_1 = \frac{\mathrm{i}kMa}{Ca\,\zeta - \mathrm{i}k/\alpha}\,\psi_1', \tag{3.4}$$

where $\zeta = 1 - c$, and all of the terms are evaluated at $y = 1$. For the jump in the normal stress component at the free surface, we obtain

$$-\mathrm{i}\psi_1''' + k(3\mathrm{i}k - Re\,\zeta)\,\psi_1' = \left[2k\,(\cot\theta - kWe) + \frac{k^3}{Ca}\right] A_1, \tag{3.5}$$

where all terms are evaluated at $y = 1$. It should be noted that in deriving (3.5) we have made use of the x-component of the linearised momentum equation (2.1) to eliminate the pressure term. The linearised kinematic equation yields

$$\psi_1 = -\zeta A_1. \tag{3.6}$$

The dynamics are governed by the Marangoni number, Ma, and also by the Reynolds number, Re, the capillary number, Ca, the Weber number, We, and the dimensionless property group α, defined by

$$Re = \frac{\rho h U_s}{\mu}, \qquad Ca = \frac{\mu U_s}{\gamma_0}, \qquad We = \frac{\varepsilon E^2 h}{2\mu U_s}, \qquad \alpha = \frac{\gamma_0 h}{\mu D_s}. \tag{3.7}$$

To determine the stability of the film, we solve (3.3) subject to (3.4)–(3.6) and compute the dimensionless growth rate of the linear perturbation, $s = kc_I$, where c_I denotes the imaginary part of the complex wave speed. Then if $s > 0$ the flow is linearly unstable and if $s < 0$ the flow is linearly stable.

4. Results

Blyth & Pozrikidis (2004*b*) used a Chebyshev-tau method to obtain numerical solutions to the linear stability problem in the absence of an electric field, with $We = 0$. They found that the flow is stable provided that the Reynolds number lies below a critical value. This critical Reynolds number decreases as the angle of inclination is increased. Studying the right-hand side of the linearized normal stress balance (3.5) we see that, for a fixed wavenumber, an electrified film at a non-zero Weber number is equivalent to a non-electrified film flowing down a wall set at the larger angle of inclination φ satisfying $\cot\varphi = \cot\theta - kWe$. In particular, if $k > We^{-1}\cot\theta$, the situation is the same as for a non-electrified film inclined at an obtuse angle to the horizontal, and physical intuition suggests that in this case, gravity is likely to have a destabilizing effect on the film flow. Following this observation, we start by considering the effect of increasing the inclination angle for a non-electrified film beyond the values discussed by Blyth & Pozrikidis (2004*b*). In figure 2, we show two neutral curves computed using the same numerical method as Blyth & Pozrikidis (2004*b*) for a contaminated film with $We = 0$ and $Ca = 2.0$, $Ma = 1.0$ and $\alpha = 10.0$. Figure 2(*a*) displays the neutral curve for a vertical film, with $\theta = 0.5\pi$, and figure 2(*b*) displays the neutral curve for a film inclined beyond the vertical, with $\theta = \cot^{-1}(-0.5) \approx 0.65\pi$. The results are in line with physical intuition which suggests that the film flow becomes less stable as the inclination angle is increased beyond the vertical. Less intuitively obvious is the presence of a hoop of stable modes penetrating the unstable region in figure 2(*b*), and which may be attributed physically to the presence of the surfactant; when the surfactant is removed, all of the modes within the hoop become unstable.

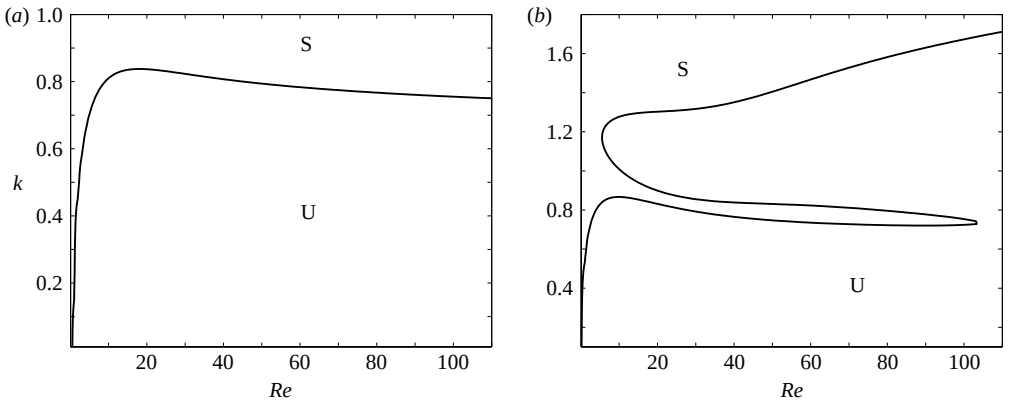

FIGURE 2. Neutral curves for a non-electrified contaminated film with $Ca = 2.0$, $Ma = 1.0$, $\alpha = 10.0$, $We = 0$ and (*a*) $\theta = 0.5\pi$, (*b*) $\theta = 0.6476\pi$. The labels *S* and *U* denote the stable and unstable regions, respectively.

Turning to an electrified film, solutions for Stokes flow may be obtained exactly by working in a similar manner to that of Pozrikidis (2003) in the absence of an electric field. The details of the calculation are provided in Appendix B. Pozrikidis showed that at zero Reynolds number there are two normal modes, both of which have a negative growth rate corresponding to a stable film. One of the modes, termed the Yih mode, is associated with the interfacial deflection, and the other, termed the Marangoni mode, is associated with the presence of the surfactant. With an electric field, when $k \gg 1$, we find the asymptote for the Yih mode,

$$s_1 \sim -\frac{1}{2Ca}k + We - (\cot\theta)\,\frac{1}{k} + \cdots, \tag{4.1}$$

and the asymptote for the Marangoni mode,

$$s_2 \sim -\frac{1}{\alpha Ca}k^2 - \frac{Ma}{2Ca}\,k + \cdots, \tag{4.2}$$

where the ... represent exponentially small terms. This shows that both modes are stable for sufficiently large wavenumber. For smaller wavenumbers, there may exist a window of unstable modes if the Weber number exceeds a critical value. The asymptotic approximations (4.1) and (4.2) agree with those of Pozrikidis (2003) when the Weber number is zero.

In figure 3(*a*), we show the growth rates, s, corresponding to the two normal modes for the case $Re = 0$, $Ca = 2.0$, $We = 1.5$, and $\alpha = 10.0$. The growth rates of the first two normal modes are shown as thin lines for a clean interface, with $Ma = 0$, and as thick lines for a contaminated interface, with $Ma = 1.0$. The asymptote (4.1) for the dominant Yih mode, s_1, is shown as a broken line in figure 3(*a*). For both small and large wavenumbers, the surfactant has little effect on the dominant growth rate. For the case with surfactant, $Ma = 1.0$, the liquid film is unstable when $1.08 < k < 5.24$ and stable otherwise. The unstable range is slightly larger for a clean interface. Figure 3(*b*) shows the effect of switching on the electric field when $Ca = 2.0$, $Ma = 1.0$, $\alpha = 10.0$ for $We = 1.5$ and $We = 0$. The growth rates of the first two normal modes are shown as thick lines for $We = 1.5$ and as thin lines for $We = 0$. When $We = 0$, the flow is stable. As can be seen, the effect of the electric field is to raise the growth rate of the first mode, provoking instability. It is noticeable that the growth rate of the second mode

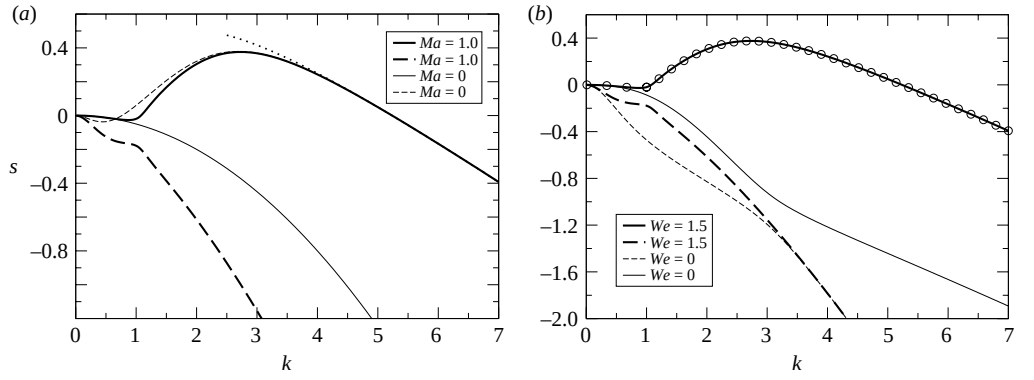

FIGURE 3. Growth rates for Stokes flow, $Re = 0$, with $Ca = 2.0$ and $\theta = \pi/4$. (*a*) $We = 1.5$, and $\alpha = 10.0$; the two most dangerous modes for $Ma = 1.0$ (thick solid and thick broken lines) and $Ma = 0$ (thin solid and thin broken lines); the dotted line indicates the asymptotic prediction (4.1). (*b*) $Ma = 1.0$ and $\alpha = 10.0$; the two most dangerous modes for $We = 1.5$ (thick solid and thick broken lines) and $We = 0$ (thin solid and thin broken lines). The circles indicate the Chebyshev-tau numerical calculations of the dominant mode for $We = 1.5$.

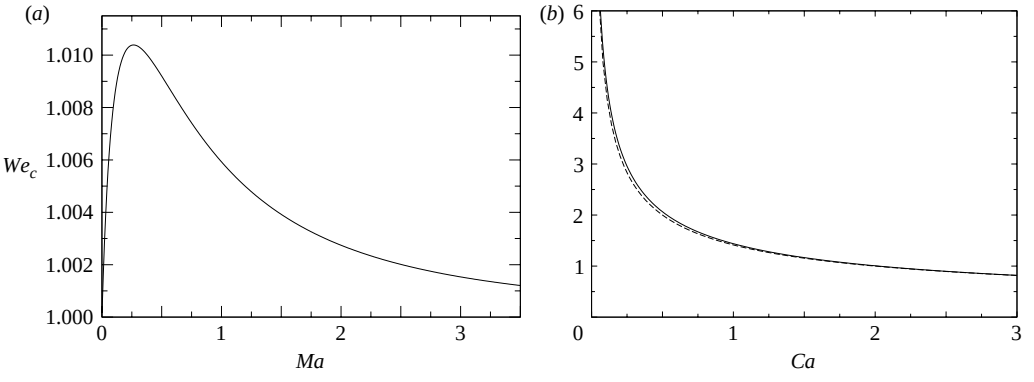

FIGURE 4. Variation of the critical Weber number, We_c, with (*a*) the Marangoni number when $Ca = 2.0$ and (*b*) with the capillary number when $Ma = 1.0$ (solid line) and $Ma = 0$ (broken line). In both (*a*) and (*b*) $\alpha = 10.0$ and $\theta = \pi/4$.

is only significantly affected over a certain range of wave-numbers. At both small and large wavenumber, the growth rate of the second mode approaches its value for an unelectrified film.

As the Weber number is reduced, the range of unstable wavenumbers contracts and disappears at a critical value, We_c, below which the film flow is stable for all wavenumbers. In figure 4, we show how this critical Weber number depends on the Marangoni and capillary numbers. Increasing the surfactant level at the fixed capillary number $Ca = 2.0$ raises the critical Weber number to a maximum value at approximately $Ma = 0.26$ (figure 4*a*). Over the range of Marangoni numbers shown, the critical wavenumber is found to vary between 2 and 2.14. Figure 4(*b*) shows the dependence of We_c on the capillary number for a contaminated film with $Ma = 1.0$, shown as a solid line, and for a clean film with $Ma = 0$, shown as a broken line. Evidently, lowering the capillary number causes We_c to increase sharply and thus

tends to stabilize the film. It is also noticeable that the presence of the surfactant has little effect on the critical Weber number.

In the absence of an electric field, the long-wave limit was studied by Benjamin (1957) and Yih (1963) for a clean free surface, and by Whitaker & Jones (1966) and Lin (1970) in the presence of surfactant. Gonzalez & Castellanos (1996) derived an expression for the growth rate of long linear waves in an electric field. With both an applied electric field and surfactant present, we expand the perturbation streamfunction ψ_1 and complex wave speed c as a series in powers of k, substitute into (3.3) and (3.4)–(3.6), and thereby derive the growth rate for long waves,

$$s = kc_I = \left(\tfrac{8}{15}Re - \tfrac{2}{3}\cot\theta - \frac{Ma}{Ca}\right)k^2 + \tfrac{2}{3}\,We\,k^3 + \cdots, \tag{4.3}$$

valid as $k \to 0$. This reduces to the result of Gonzalez & Castellanos (1996) when $Ma = 0$. The electric field only affects the growth rate of long-wave disturbances at second order. It introduces a first-order correction to the critical Reynolds number reported by Blyth & Pozrikidis (2004*b*) for instability,

$$Re_c = \tfrac{5}{4}\cot\theta + \frac{15Ma}{8\,Ca} - \tfrac{5}{4}\,We\,k. \tag{4.4}$$

In line with the observations of Gonzalez & Castellanos (1996), the electric field correction reduces the critical Reynolds number, introducing a band of unstable modes for $Re > Re_c$. This highlights the destabilizing effect of the electric field. It should be noted, however, that (4.4) only represents the critical Reynolds number when the Weber number is below a threshold value. As we shall see below, the neutral curve may turn back on itself further up in wavenumber space and so produce instability at a lower Reynolds number. This is in accord with the above comments regarding Stokes flow, where for sufficiently large Weber number, instability occurs at zero Reynolds number.

For general parameter values, the problem (3.3)–(3.6) must be solved numerically. Kim *et al.* (1991) presented some results for an infinite electrode placed at a large, but finite distance from a clean film. They used a shooting method to compute results for quite small wavenumbers and Reynolds numbers up to 20. We have computed results using the Chebyshev-tau method of Blyth & Pozrikidis (2004*b*) modified to include the effect of the electric field in the normal stress condition. The method is capable of producing highly accurate solutions for a wide range of Reynolds numbers up to very large values. By way of a check on the results, in figure 3(*b*) we show the computed growth rate of the dominant normal mode for the case $Ca = 2.0$, $Ma = 1.0$, $\alpha = 10.0$, and $We = 1.5$. The results computed using the Chebyshev-tau method are shown as circles. The predictions of the Stokes analysis are shown as a solid line. The agreement between the two sets of results is excellent. Here and in the remainder of the paper, results were computed using 25 Chebyshev modes, which are sufficient to produce an accurate solution.

We begin by considering the effect of an electric field on a clean film. In figure 5 ($a-d$), we show the neutral curves separating stable and unstable modes in the (Re, k)-plane for a clean film with $Ma = 0$ when $Ca = 2.0$. The neutral curve when there is no electric field, $We = 0$ shown in figure 5(*a*) is identical to that found by Blyth & Pozrikidis (2004*b*) in their figure 5(*a*). The portions of the curves below about $k = 0.8$ agree qualitatively in shape with those presented by Kim *et al.* (1991) in their figure 2 for different parameter values. The results of Blyth & Pozrikidis (2004*b*) show that the Marangoni mode dominates in the stable region, and the Yih mode

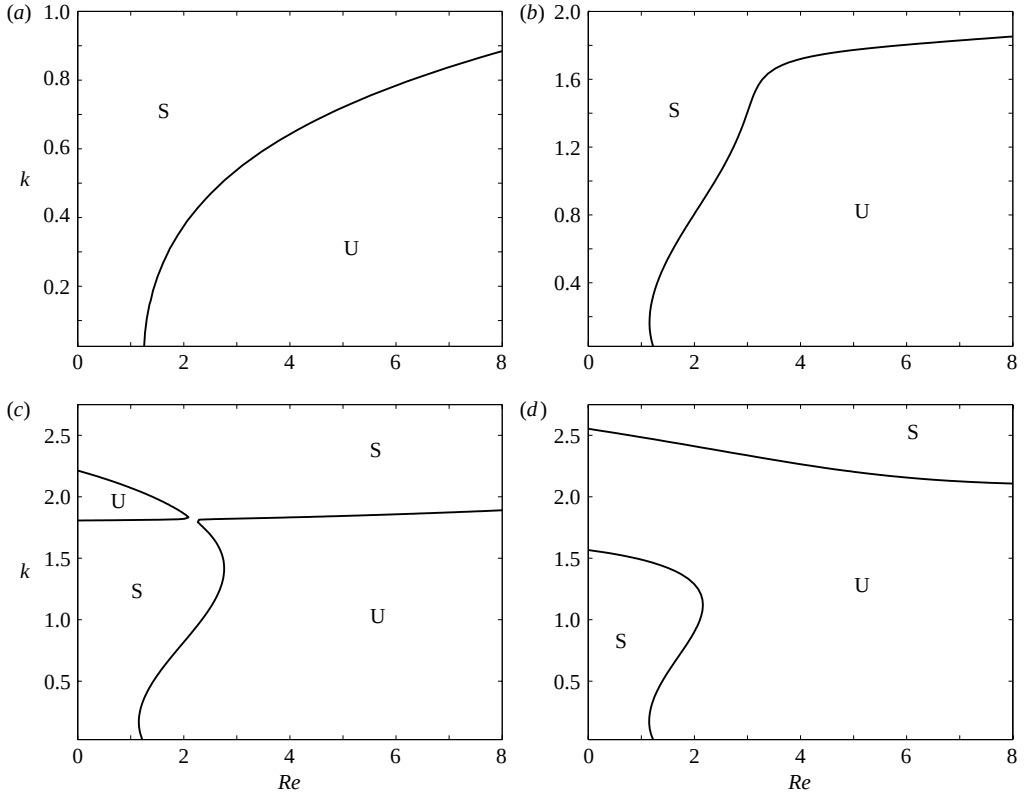

FIGURE 5. Neutral curves for a clean film with $Ma = 0$, $Ca = 2$ and $\theta = \pi/4$ for (*a*) $We = 0$, (*b*) $We = 1.0$, (*c*) $We = 1.0052$, (*d*) $We = 1.03$. The labels S and U denote the stable and unstable regions, respectively.

dominates in the unstable region; see in particular their figure 4(*a*). The same applies in the presence of an electric field. A numerical check on the size of the individual terms in the normal and tangential stress balances, (3.4) and (3.5), confirms that, for a fixed wavenumber in figure 5(*b*), where $We = 1.0$, the surfactant plays a dominant role in the stable region, but takes a back-seat role in the unstable region.

As the Weber number is increased, the small wavenumber portion of the neutral curves in figure 5 is tugged towards the k-axis while the critical Reynolds number, Re_c, for instability decreases in accordance with (4.4). The analysis for Stokes flow shows that when $Ca = 2$, the critical Weber number for instability at zero Reynolds number is given by $We_c = 1$ (see figure 4*b*) with corresponding critical wavenumber $k_c = 2$. For $We > 1$, the neutral curves cut the k-axis subtending a window of unstable modes at $Re = 0$ around $k = k_c$. The result for $We = 1.0052$ (figure 5*c*) indicates how the topology of the curves changes as the Weber number is increased beyond the critical unit value. As We increases above 1.0052, the two curves in figure 5(*c*) merge and then split apart to form an upper and a lower branch. These branches are illustrated for the sample case $We = 1.03$ in figure 5(*d*). The lower and upper branches cut the vertical axis at $k = 1.57$ and $k = 2.55$, respectively, in agreement with exact calculations for Stokes flow following the description in Appendix B. The lower branches of the neutral curves for larger Weber number are shown in figure 6. The upper branches, which are not shown, are shifted upwards to larger and larger wavenumbers as We increases.

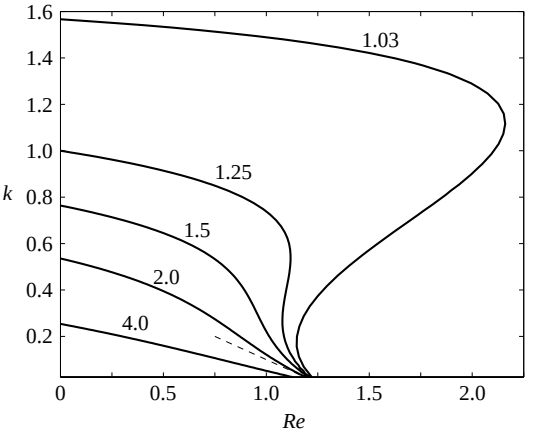

FIGURE 6. The lower branches of the neutral curves for a clean film with $Ma = 0$ and $Ca = 2$ for $We = 1.03$, 1.25, 1.5, 2.0, 4.0 as shown. The broken line indicates the predicted critical Reynolds number (4.4) when $We = 2.0$.

For a fixed Weber number and a sufficiently large wavenumber perturbation, the film is stable. As in figure 5(*d*), each lower branch curve encloses a region of stable modes including the origin. Points outside of this region (but beneath the unseen upper branch) correspond to unstable modes. As *We* increases, the cut-off wavenumber at $Re = 0$ decreases and the region of stable modes shrinks progressively. The broken line indicates the long-wave prediction (4.4) when $We = 2.0$.

The behaviour of the neutral curves as the Weber number varies is markedly different when surfactant is present. Blyth & Pozrikidis (2004*b*) found that for a contaminated film with no electric field, the critical Reynolds number increases monotonically with the wavenumber for acute inclination angles. As discussed above, imposing an electric field for a fixed wavenumber perturbation may alternatively be viewed as increasing the angle of inclination, θ, for a non-electrified film. We saw in figure 2(*b*) how increasing the angle of inclination leads the neutral curve to follow a more complicated path. Consequently, we should expect the electric field to have a significant effect on the shape of the neutral curves. Neutral curves for a contaminated film subjected to an electric field are shown in figure 7 for $Ca = 2.0$, $Ma = 1.0$, $\alpha = 10.0$, $\theta = \pi/4$ and a sequence of values of *We*. The Stokes flow analysis yields the critical Weber number $We_c = 1.006$ when $Ma = 1.0$ and $Ca = 2.0$. The neutral curve corresponding to this critical value is shown in figure 7(*a*). When $We < We_c$, the critical Reynolds number is computed to be $Re_c \approx 2.2$ in agreement with the predicted value $Re_c = 2.1875$ from (4.4). When $We > We_c$, there appears a small neutral hoop subtending a window of unstable modes at zero Reynolds number (figure 7*b*). As *We* increases, the gap between the hoop and the original branch closes and the two pinch together and then separate to form distinct upper and lower neutral branches (figure 7*c*). A long finger of stable modes on the lower branch protrudes up to about $Re = 218$ at the tip when $We = 1.1$. As the Weber number is further increased, the upper branch moves upwards, widening the band of unstable modes at $Re = 0$. The length of the lower neutral 'finger' shortens with increasing Weber number. Figure 8 shows that when $We \approx 1.85$, the lower branch finger pinches together to leave an isolated loop of stable modes displayed in figure 9(*a*). The upper branches in figures 8 and 9(*a*) emanate from $k = 6.81$ and $k = 7.46$ at $Re = 0$, respectively, but are not

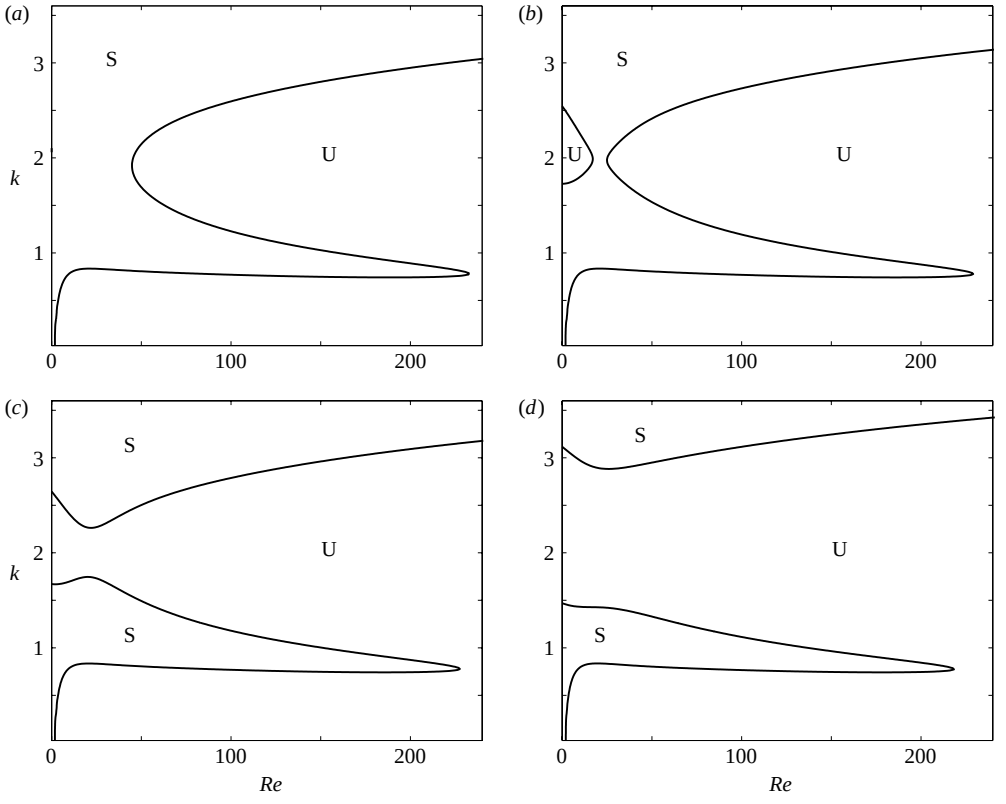

FIGURE 7. Neutral curves for the case $Ca = 2.0$, $Ma = 1.0$, $\alpha = 10.0$, $\theta = \pi/4$ and (*a*) $We = 1.006$, (*b*) $We = 1.03$, (*c*) $We = 1.04$, (*d*) $We = 1.1$. The labels S and U denote the stable and unstable regions, respectively.

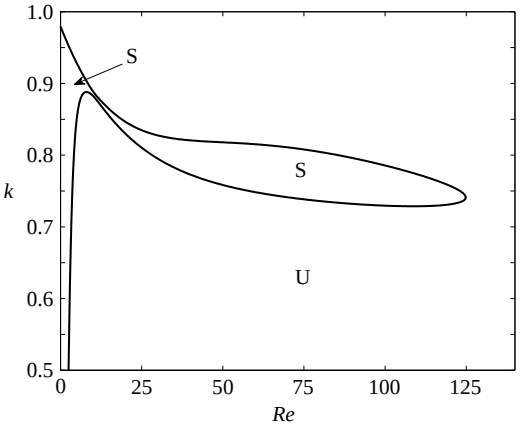

FIGURE 8. The pinching of the lower branch of the neutral curve for $Ca = 2.0$, $Ma = 1.0$, $\alpha = 10.0$ and $We = 1.85$. The labels S and U denote the stable and unstable regions, respectively.

shown. As the Weber number increases, the upper branches move upwards to larger and larger wavenumbers; for sufficiently large wavenumber, the flow is stable. The appearance of the stable loop is anticipated by the results shown in figure 2(*b*) where the appearance of a loop of stable modes was demonstrated for a non-electrified

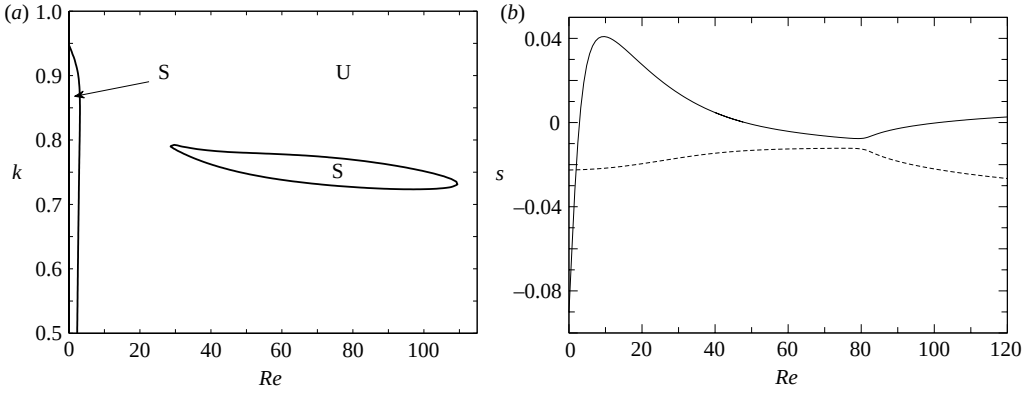

FIGURE 9. The case $Ca = 2.0$, $Ma = 1.0$, $\alpha = 10.0$, $\theta = \pi/4$ and $We = 2.0$: (*a*) the lower branches of the neutral curve, and (*b*) the variation of the growth rates of the Yih mode, shown as a broken line, and the Marangoni mode, shown as a solid line, with Reynolds number when $k = 0.75$.

film on a wall inclined beyond the vertical. Figure 9(*b*) shows the effect of inertia on the growth rates of the Yih and Marangoni modes, which in this case correspond to the two most dangerous modes, at the fixed wavenumber $k = 0.75$. The Yih mode dominates at very small Reynolds number, but is rapidly overtaken by the Marangoni mode, which governs the stability at higher Reynolds number and through the stable loop seen in the neutral curve of figure 9(*a*). Checking the numerical size of the individual terms in the normal and tangential stress balances (3.4) and (3.5) confirms that the surfactant has little effect at small Reynolds number, but plays a dominant role at moderate to large Reynolds number.

To provide a guideline calculation for the stability of a liquid film under laboratory conditions, we select the physical parameter values used by Wierschem, Scholle & Aksel (2003) in their experiments on film flow down a corrugated wall. They took $h = 0.5\,\mathrm{cm}$, $\gamma = 21.4\,\mathrm{g\,cm^{-2}}$, $\rho = 0.972\,\mathrm{g\,cm^{-3}}$ and $\mu = 56.2\,\mathrm{g\,cm^{-1}s^{-1}}$, which yield equivalent values of the Reynolds number and capillary number for a flat wall inclined at an angle $\theta = \pi/4$ to the horizontal of $Re = 0.013$ and $Ca = 4.0$. Typical values for the Marangoni number and surfactant diffusivity at an air–water interface are given by $Ma = 0.02$ and $D_s = 10^{-6}\,\mathrm{cm^2\,s^{-1}}$ (Eggleton, Pawar & Stebe 1999, p. 87). With this value for the surfactant diffusivity we find $\alpha = 2 \times 10^5$. Under these conditions, when there is no electric field, $We = 0$, the film is stable. The critical Weber number for instability is $We_c \approx 0.71$, corresponding to a critical electric field strength of $E_0 = 1.64 \times 10^4\,\mathrm{V\ cm^{-1}}$. For Weber numbers beyond this value the film is unstable.

5. Discussion

We have studied the linear stability of a liquid film flowing down an inclined plane when the film surface is contaminated with an insoluble surfactant and the film is subjected to an electric field. The problem was formulated for arbitrary parameter values. Exact solutions to the linear stability problem were presented at zero Reynolds number, and a Chebyshev-tau numerical method was used to compute results at finite Reynolds number.

At zero Reynolds number, there exists a critical Weber number above which the film becomes unstable. Increasing the Weber number through and beyond this critical

value opens up a window of unstable modes subtended about a critical wavenumber. Below the critical Weber number, the flow is stable. For large wavenumber, regardless of the size of the Weber number, the flow is stable and to leading order, the first two normal modes behave as they would with no applied electric field. The critical Weber number has only a mild dependence on the Marangoni number, varying typically by only about 1% as the Marangoni number is increased from zero. However, the critical Weber number shows a much stronger dependence on the capillary number. In particular, the critical Weber number increases without bound as the capillary number is lowered.

When the Reynolds number exceeds a threshold value, the film is always unstable for sufficiently small wavenumber. The stability characteristics for larger wavenumber depend crucially on the size of the Weber number. In addition, the stability characteristics are significantly different for a clean and a contaminated film subjected to an electric field. With no surfactant present, the neutral curve consists of a single branch extending like a parabola from a finite critical Reynolds number at $k = 0$. The critical Reynolds number gradually decreases as the Weber number is increased. It jumps to zero at a particular value of the Weber number when a hoop of unstable modes centred around a critical wavenumber emerges from $Re = 0$. The hoop makes contact with the original branch and the two then separate to form two disjoint branches, an upper and a lower, sandwiching unstable modes in between. With surfactant present, the neutral curve at zero Weber number is similar to that found for a clean film, but deformed to include a long finger of stable modes penetrating to a large Reynolds number. As the Weber number is raised, a hoop of unstable modes again emerges from $Re = 0$ and connects with the main curve to form an upper branch and a lower branch. Ultimately, the long finger which now forms the main part of the lower branch pinches off to leave a disjoint island of stable modes isolated in parameter space.

In conclusion, we affirm the results of previous studies that the electric field has a destabilizing influence on the film dynamics. In particular, it tends to lower the critical Reynolds number for instability at a given wavenumber. The introduction of surfactant onto the electrified film has important implications for the topology of the neutral curves in wavenumber/Reynolds number space. In particular, the surfactant is able to stabilize the flow for a set of modes which would otherwise be unstable for a clean electrified film.

This research was supported by the EPSRC under grant EP/D052289/1.

Appendix A. Squire's transformation for film flow

Yih (1955) discussed the extension of Squire's theorem to free-surface flows, but did not present explicit details. Hesla, Pranckh & Preziosi (1986) considered the case of two superposed clean fluid layers of different viscosity and density in a channel. Here we demonstrate that it is possible to extend Squire's transformation to the currently considered problem of film flow down an inclined plane in the presence of an insoluble surfactant and a normal electric field.

The problem is to solve the linearized form of (2.1) valid for a small three-dimensional disturbance to the basic flow. The boundary conditions include the no-slip and impermeability conditions at the wall, and at the free surface the kinematic condition and the dynamic stress condition,

$$\boldsymbol{\sigma} \cdot \boldsymbol{n} = -(2\gamma\kappa_m + p_a)\,\boldsymbol{n} - \nabla_s \gamma - \boldsymbol{M} \cdot \boldsymbol{n}, \tag{A 1}$$

where $\nabla_s = (\boldsymbol{I} - \boldsymbol{nn}) \cdot \nabla$ is the surface gradient operator acting in a plane tangential to the free surface, and $\kappa_m \equiv (1/2)\nabla \cdot \boldsymbol{n}$ is the mean curvature. The surfactant transport equation is (e.g. Li & Pozrikidis 1997; Yon & Pozrikidis 1998)

$$\frac{\mathrm{d}\Gamma}{\mathrm{d}t} + \nabla_s \cdot (\Gamma \boldsymbol{u}_s) = -2\Gamma\kappa_m \boldsymbol{u} \cdot \boldsymbol{n} + D_s \nabla_s^2 \Gamma, \tag{A 2}$$

where $\boldsymbol{u}_s = (\boldsymbol{I} - \boldsymbol{nn}) \cdot \boldsymbol{u}$ is the surface velocity. The derivative $\mathrm{d}/\mathrm{d}t$ is defined in § 2. The Gibbs' linear law relating the surface tension to the local surfactant concentration is given by (2.8). The electric field problem is given by (2.6) with $\phi = 0$ on the free surface and with $\phi \to -Ey$ as $y \to \infty$.

We non-dimensionalize as described in § 3 and assume that the film is perturbed so that the free surface is located at

$$y = 1 + \delta\, A_1\, \mathrm{e}^{\mathrm{i}(kx+mz-kct)}, \tag{A 3}$$

where m is the transverse wavenumber and the z-axis points out of the paper in figure 1. The velocity field, pressure, surface tension and surfactant concentration are expanded as

$$\begin{aligned} (u,\ v,\ w) &= (2y - y^2,\ 0,\ 0) + \delta\,(u_1(y),\ v_1(y),\ w_1(y))\,\mathrm{e}^{\mathrm{i}(kx+mz-kct)} + \cdots, \\ p &= p_a/\left(\rho U_s^2\right) + 2Re^{-1}(1-y)\cot\theta + \delta\, p_1(y)\,\mathrm{e}^{\mathrm{i}(kx+mz-kct)} + \cdots, \\ (\gamma,\ \Gamma,\ \phi) &= (1,\ 1,\ -y) + \delta\,(\gamma_1,\ \Gamma_1,\ \phi_1)\,\mathrm{e}^{\mathrm{i}(kx+mz-kct)} + \cdots, \end{aligned} \tag{A 4}$$

where w is the velocity component in the z-direction. Substituting the expansions for the velocity field and pressure into the dimensionless form of (2.1) and linearizing, we derive a standard set of perturbation momentum equations, with body force terms due to gravity, governing three-dimensional disturbances (e.g. Drazin & Reid, p. 155).

The no-slip and impermeability conditions at the wall require $u_1 = v_1 = w_1 = 0$. At the free surface, we define $\boldsymbol{t}_x$ to be the unit vector tangent to the surface pointing in the x-direction, and $\boldsymbol{t}_z$ to be the binormal unit vector satisfying $\boldsymbol{t}_z = \boldsymbol{t}_x \times \boldsymbol{n}$. Next, we substitute (A 4) into the dimensionless form of (A 1), linearize, and take the normal component to obtain

$$A_1 \left(2\cot\theta + \frac{k^2+m^2}{Ca}\right) - Re\ p_1 + 2v_1' + 2We\,\phi_1' = 0, \tag{A 5}$$

and the $\boldsymbol{t}_x$ component to obtain

$$2A_1 - u_1' - \mathrm{i}k\, v_1 = 2\,\mathrm{i}kWe\,(A_1 + \phi_1) - \frac{\alpha k\,(ku_1 + mw_1)\,Ma}{\mathrm{i}\alpha Ca\ k(c-1) - (k^2+m^2)}, \tag{A 6}$$

and the $\boldsymbol{t}_z$ component to obtain

$$-\mathrm{i}mv_1 - w_1' = 2\,\mathrm{i}mWe\,(A_1 + \phi_1) - \frac{\alpha m\,(ku_1 + mw_1)\,Ma}{\mathrm{i}\alpha Ca\ k(c-1) - (k^2+m^2)}. \tag{A 7}$$

The kinematic condition becomes

$$v_1 + \mathrm{i}kA_1\,(c-1) = 0. \tag{A 8}$$

All terms in (A 5)–(A 8) are evaluated at $y = 1$. Defining an extended form of Squire's transformation (e.g. Drazin & Reid, p. 129, 155), we write $\tilde{k}^2 = k^2 + m^2$, $\tilde{c} = c$, and $\tilde{k}\tilde{Re} = kRe$, $\tilde{k}\tilde{Ca} = kCa$, $k\tilde{We} = \tilde{k}We$, together with

$$\left.\begin{aligned} &\tilde{k}\tilde{A}_1 = kA_1, \qquad \tilde{k}\tilde{u}_1 = ku_1 + mw_1, \qquad \tilde{v}_1 = v_1, \\ &k\tilde{p}_1 = \tilde{k}p_1 + 2\,(A_1/Re)(k - \tilde{k})\cot\theta, \qquad \tilde{k}\tilde{\phi}_1 = k\phi_1. \end{aligned}\right\} \tag{A 9}$$

Transforming the governing system for the three-dimensional problem, we recover the system governing the development of two-dimensional disturbances of wavenumber $\tilde{k}$ and complex wave speed $\tilde{c}$. For example, (A 5), (A 6) and (A 8) reduce to their current forms with w_1 and m set to zero and with k replaced by $\tilde{k}$. Accordingly, to determine the critical Reynolds number for instability it is sufficient to consider only two-dimensional perturbations.

Appendix B. Stokes flow analysis

In this Appendix, we give brief details of the linear stability calculation for Stokes flow. The details represent a modification of the analysis presented by Pozrikidis (2003), who examined film flow down an inclined plane in the presence of surfactant. The present modification allows for the inclusion of an electric field.

At zero Reynolds number, the problem to be solved is given by (3.3)–(3.6), but with the right-hand side of (3.3) set to zero. Integrating (3.3), we obtain

$$\psi_1(y) = a_1 e^{ky} + a_2 y e^{ky} + a_3 e^{-ky} + a_4 y e^{ky}. \tag{B 1}$$

The impermeability condition at $y=0$ yields $a_3 = -a_1$ and the kinematic condition (3.6) yields $A_1 = -\psi_1(1)/\zeta$. Compiling the remaining boundary conditions, we derive the matrix system $\boldsymbol{Q}\cdot\boldsymbol{x}=0$, where

$$\boldsymbol{Q} = \boldsymbol{N} + \mathrm{i}kWe \begin{pmatrix} 0 & 0 & 0 & 0 \\ 0 & 0 & 0 & 0 \\ 1-q & 1 & q & 0 \\ 0 & 0 & 0 & 0 \end{pmatrix}, \tag{B 2}$$

and $\boldsymbol{x} = (a_1, a_2, a_4, \gamma_1)^T$. The matrix $\boldsymbol{N}$ is given in (4.2) of Pozrikidis (2003) but with, in the notation of that paper, Ca replaced by Ca' and Pe replaced by $2\pi\alpha' Ca'/k$. Note that Pozrikidis' definitions of Ca' and α' coincide with the current definitions of Ca and α, respectively. For non-trivial solutions, we require $\det(\boldsymbol{Q})=0$ which yields a cubic equation with the trivial solution $\zeta=0$ and two non-trivial solutions. The latter two solutions correspond to two normal modes, as was found by Pozrikidis (2003).

REFERENCES

Adamson, A. W. 1990 *Physical Chemistry of Surfaces*. Wiley.

Anshus, B. E. & Acrivos, A. 1967 The effect of surface-active agents on the stability characteristics of falling liquid films. *Chem. Engng Sci.* **22**, 389–393.

Benjamin, T. B. 1957 Wave formation in laminar flow down an inclined plane. *J. Fluid Mech.* **2**, 554–574.

Benjamin, T. B. 1964 Effect of surface contamination on wave formation in falling liquid films. *Archwm. Mech. Stosow.* **16**, 615–626.

Blyth, M. G. & Pozrikidis, C. 2004*a* Effect of surfactants on the stability of two-layer channel flow. *J. Fluid Mech.* **505**, 59–86.

Blyth, M. G. & Pozrikidis, C. 2004*b* Effect of surfactant on the stability of film flow down an inclined plane. *J. Fluid Mech.* **521**, 241–250.

Blyth, M. G. & Pozrikidis, C. 2004*c* Effect of inertia on the Marangoni instability of the two-layer channel flow. Part II. Normal-mode analysis. *J. Engng Maths.* **50**, 329–341.

Drazin, P. G. & Reid, W. H. 1981 *Hydrodynamic Stability*. Cambridge University Press.

Dukler, A. 1976 The role of waves in two phase flow: some new understanding. *Chem. Engng Educ.* Summer, 108–138.

Eggleton, C. D., Pawar, Y. P. & Stebe, K. J. 1999 Insoluble surfactants on a drop in an extensional flow: a generalization of the stagnated surface limit to deforming interfaces. *J. Fluid Mech.* **385**, 79–99.

Frenkel, A. L. & Halpern, D. 2002 Stokes flow instability due to interfacial surfactant. *Phys. Fluids* **14**, 45–48.

Frenkel, A. L. & Halpern, D. 2005 Effect of inertia on the insoluble-surfactant instability of a shear flow. *Phys. Rev.* E **71**, 016302.

Gonzalez, A. & Castellanos, A. 1996 Nonlinear electrohydrodynamic waves on films falling down an inclined plane. *Phys. Rev.* E **53**, 3573–3578.

Griffing, E. M., Bankhoff, S. G., Miksis, M. J. & Schluter, R. A. 2006 Electrohydrodynamics of thin flowing films. *Trans. ASME* I: *J. Fluids Engng* **128**, 276–283.

Ha, J.-W. & Yang, S.-M. 1995 Effects of surfactant on the deformation and stability of a drop in a viscous fluid in an electric field. *J. Colloid Interface Sci.* **175**, 369–385.

Ha, J.-W. & Yang, S.-M. 1998 Effect of nonionic surfactant on the deformation and breakup of a drop in an electric field. *J. Colloid Interface Sci.* **206**, 195–204.

Halpern, D. & Frenkel, A. L. 2003 Destabilization of a creeping flow by interfacial surfactant: linear theory extended to all wavenumbers. *J. Fluid Mech.* **485**, 191–220.

Hesla, T. I., Pranckh, F. R. & Preziosi, L. 1986 Squire's theorem for two stratified fluids. *Phys. Fluids* **29**, 2808–2811.

Ji, W. & Setterwall, F. 1994 On the instabilities of vertical falling liquid films in the presence of surface-active solute. *J. Fluid Mech.* **278**, 297–323.

Karniadakis, G., Beskok, A. & Aluru, N. 2005 *Microflows and Nanoflows*. Springer.

Kim, H., Bankoff, S. G. & Miksis, M. J. 1991 The effect of an electrostatic field on film flow down an inclined plane. *Phys. Fluids* A**4**, 2117–2130.

Kistler, S. F. & Schweizer, P. M. 1997 *Liquid Film Coating*. Chapman & Hall.

Li, X. F. & Pozrikidis, C. 1997 The effect of surfactants on drop deformation and on the rheology of dilute emulsions in Stokes flow. *J. Fluid Mech.* **341**, 165–194.

Lin, S. P. 1970 Stabilizing effects of surface-active agents on a film flow. *AIChE* **16**, 375–379.

Matar, O. K. & Lawrence, C. J. 2006 The flow of a thin conducting film over a spinning disc in the presence of an electric field. *Chem. Engng Sci.* **61**, 3838–3849.

Melcher, J. R. & Taylor, G. I. 1969 Electrohydrodynamics: a review of the role of interfacial shear stresses. *Annu. Rev. Fluid Mech.* **1**, 111–146.

Mukhopadhyay, A. & Dandapat, B. S. 2005 Nonlinear stability of a conducting viscous film flowing down an inclined plane at moderate Reynolds number in the presence of a uniform normal electric field. *J. Phys.* D **38**, 138–143.

Pozrikidis, C. 2003 Effect of surfactants on film flow down a periodic wall. *J. Fluid Mech.* **496**, 105–127.

Pozrikidis, C. 2004 Instability of multi-layer channel and film flows. *Adv. Appl. Mech.* **40**, 179–239.

Shen, M. C., Sun, S. M. & Meyer, R. E. 1991 Surface waves on viscous magnetic fluid flow down an inclined plane. *Phys. Fluids* A**3**, 439–445.

Tseluiko, D. & Papageorgiou, D. T. 2006 Wave evolution on electrified falling films. *J. Fluid Mech.* **556**, 361–386.

Weinstein, S. J. & Ruschak, K. J. 2004 Coating flows. *Annu. Rev. Fluid Mech.* **36**, 29–53.

Wierschem A., Scholle, M. & Aksel, N. 2003 Vortices in film flow over strongly undulated bottom profiles at low Reynolds numbers. *Phys. Fluids* **15**, 426–435.

Whitaker, S. 1964 Effect of surface active agents on the stability of falling liquid films. *Ind. Engng Chem. Fundls* **3**, 132–142.

Whitaker, S. & Jones, L. O. 1966 Stability of falling liquid films. Effect of interface and interfacial mass transport. *AIChE* **12**, 421–431.

Yih, C. S. 1955 Stability of two-dimensional parallel flows for three-dimensional disturbances. *Q. Appl. Maths.* **12**, 434–435.

Yih, C. S. 1963 Stability of a liquid flow down an inclined plane. *Phys. Fluids* **6**, 321–334.

Yon, S. & Pozrikidis, C. 1998 A finite-volume/boundary-element method for flow past interfaces in the presence of surfactants, with application to shear flow past a viscous drop. *Comput. Fluids* **27**, 879–902.

Yoshimura, P., Nosoko, T. & Nagata T. 1996 Enhancement of mass transfer into a falling laminar liquid film by two-dimensional surface waves – some experimental observations and modeling. *Chem. Engng Sci.* **51**, 1231–1240.